An Ionic Transfer Investigation of Tri-Iodine of Solvent-Free Oligomeric Electrolytes in Dye-Sensitized Solar Cells

Fu-Ming Wang[1,], Chia-Hsien Chu[2], Chia-Hua Lee[3], Jia-Yin Wu[3], Kun-Mu Lee[3], Yung-Liang Tung[3], Chang-Ho Liou[4], Yung-Yun Wang[2] and Chi-Chao Wan[2]*

[1] Nanoelectrochemistry Laboratory, Graduate Institute of Engineering, National Taiwan University of Science and Technology, Taipei, Taiwan
[2] Department of Chemical Engineering, National Tsing Hua University, Hsinchu, Taiwan
[3] Photovoltaics Technology Center, Industrial Technology Research Institute, Chutung, Hsinchu, Taiwan
[4] Electronics & Optoelectronics Research Laboratories Industrial Technology Research Institute, Chutung, Hsinchu, Taiwan
[*]E-mail: mccabe@mail.ntust.edu.tw

A series of novel solvent-free oligomeric electrolytes based on poly (ethyl glycol) methyl ether methacrylate for dye-sensitized solar cells (DSSCs) are currently under development. The aim of this study was to investigate the effects of tri-iodine (I_3^-) ionic transport on the side-chain length of ethylene-oxide (EO), and its overall influence on the performance of dye-sensitized solar cells. Solvent-free oligomeric electrolytes with EO side chains of the shortest length enhanced the diffusion coefficient of I_3^-, thereby promoting redox reactions in DSSCs, and increasing the short circuit current density (J_{sc}). In addition, free volume measurements of oligomeric electrolytes provided a possible explanation regarding the ionic transfer mechanism and a conceptual framework related to the influence of the length of the EO side chain. Finally, a 30-day long-running test demonstrated that these oligomer systems are robust and stable. The current-voltage (I-V) characteristics of the oligomeric electrolyte produced the best results, with values of 0.62 V for V_{oc}, 9.71 mA cm^{-2} for J_{sc}, 0.59 for fill factor (FF), and 3.56% cell efficiency under AM 1.5.

1. INTRODUCTION

Dye-sensitized solar cells (DSSCs) have been attracting a great deal of interest in the field of photo-electrochemistry, owing to their high photoelectric conversion efficiency and low production costs, compared to conventional silicon-based solar cells [1-3]. In 1991, Professor Gratzel first

described the concept of dye-sensitization, using a Ruthenium bipyridyl complex, with acetonitrile (AN) ligands, achieving a conversion efficiency of 10-11% [4]. Unfortunately, high efficiency solar cells must operate under ambient sunlight conditions, suggesting that volatile liquid electrolytes are at risk of evaporation, and that long-term operation of the devices may lead to high operating temperatures [5]. These factors could result in damage to the solar cells, with a corresponding risk to human health. Polymer electrolytes are an attractive alternative, and during the past decade scientists have been paying particular attention to poly (ethylene oxide) PEO, due to its non-volatile performance as a solvent free, gel-polymer (quasi-solid) electrolyte in both lithium ion batteries [6, 7], and DSSCs [8, 9]. However, PEO has poor conductivity ($\sigma \sim 10^{-7}$ S/cm) due to the high degree of crystallinity it exhibits at ambient temperatures. Several measures have been attempted to overcome this problem, including the use of metal oxides, Al_2O_3, TiO_2, and SiO_2, as a replacement for PEO [10-13], as well as atactic poly (propylene oxide) (PPO) randomly copolymerized with ethylene oxide (EO) [14]. However, these alternatives present problems associated with poor ionic conductivity, and difficulty of manufacture. Employing an oligomeric electrolyte could help to overcome the above problems of highly viscous polymer electrolytes, which restrict ionic conductivity due to their high molecular weight. Recently, Lee *et al*. [15] carried out research in this area using poly (ethyleneglycol) dimethyl ether (PEGDME) mixed with 1-methyl-3-propylimidazolium as a binary oligomeric electrolyte, achieving a conversion efficiency of 5%. In that report, Lee also discussed the diffusion coefficients of I^- and I^{3-} as a function of the molecular weight of the oligomer. Non-flammable, room temperature ionic liquids (RTIL) are another attractive alternative, particularly in light of the safety aspect, which could very well outweigh conversion efficiency when considering available alternatives [16, 17]. Unfortunately, RTIL production costs are far higher than those of organic liquid electrolytes are. With this in mind, we selected DSSCs with oligomeric electrolytes as the concept with the greatest potential, due to its freedom from volatile organic compounds, its high ionic conductivity, and low manufacturing costs. The goal of this study therefore, was the development of an appropriate oligomeric electrolyte for use with DSSCs. The primary factors that had to be taken into consideration were conformational flexibility, ionic conductivity, and migratory movement of the I_3^-, tri-iodide ions through these oligomeric electrolytes.

In a study of lithium ion batteries, Wang *et al.* [18-20] identified a crucial relationship between the behavior of lithium-ion migration and the bulk structure of the electrolyte. Ionic transfer rates vary in solid polymers and carbonate liquid electrolytes. This study evaluated the means by which electron-withdrawing groups (present on the backbone of polymers), influence the hopping mechanism that facilitates ionic transport. Additionally, EO side-chain vibrations and conformational motion varies according to length of the chain, influencing the entire polymer free volume, which in turn, provides a route for ionic transfer. Wang *et al.* named this ionic transfer phenomenon "The combination dual effect of ionic transformation in a solid polymer electrolyte system". Ionic motion in liquid electrolytes on the other hand, owes more to viscosity and the dielectric constant [21, 22]. As a follow up of this research, Wang *et al.* fabricated a series of chemical composite films, to enhance the ionic diffusion in lithium ion batteries.

In this study, we developed, a novel solvent-free, oligomeric electrolyte system doped with the ionic liquid 1-methyl-3-propylimidazolium iodide (PMII). We then compared our oligomer/PMII

system a binary ionic liquid system using EMIBCN/ PMII, reported by Michael Grätzel [23]. The oligomer used in this research was poly (ethyl glycol) methyl ether methacrylate (PEGMEMA), containing an ethylene-oxide (EO) group, capable of trapping lithium ions, and forming a matrix capable of incorporating salts, without the assistance of additional solvents. During our studies of electrolytes, we investigated the effects of oligomer side-chains of various molecular weights to observe their effects on ambient ionic conductivity, bulk viscosity, tri-iodide ionic motion, free volume effects, and the performance of solar cells.

2. EXPERIMENTAL

2.1. Materials

Poly (ethyl glycol) methyl ether methacrylate (PEGMEMA) (Scheme 1) of three different molecular weights, 475, 300 and 188 g mole^{-1}, was purchased from Sigma Aldrich (>99%). It was used as the host material doped with 1-methyl-3-propylimidazolium iodide (PMII), an ionic liquid, purchased from Merck (>99%), which in turn was used as an iodide source in a ratio of 7:13 (v/v).
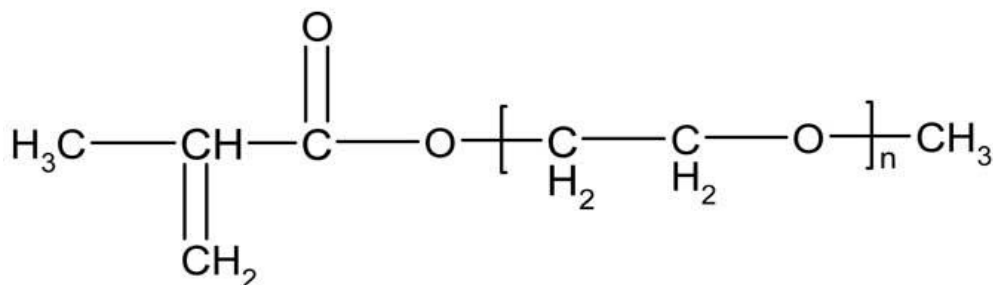
oligomer no.	1	2	3
n	2	4.5	8.5

Scheme 1. The structure of PEGMEMA oligomeric electrolytes with various EO side chains.

Each oligomeric electrolyte is referred to as PEGMEMA$_{188}$ (oligomer 1), PEGMEMA$_{300}$ (oligomer 2), and PEGMEMA$_{475}$ (oligomer 3). *N*-methyl benzyl imidazolium (NMBI), was purchased from Sigma Aldrich (>99%), for use as an additive reagent. All compounds were used directly, without further purification.

2.2. Viscosity analysis

Rheological characterization of the oligomeric electrolytes was determined with an Advanced Rheometer AR 2000 (TA Instrument). This instrument included a feedback control device, to measure

the viscosity of polymers across a wide range of sheer rates over a period of time at a particular fixed temperature.

2.3. Electrochemical measurements

An ultra-microelectrode technique with Pt counter and Pt reference electrodes has frequently been used to measure ionic diffusion coefficients of I^{3-}, which are directly connected with the redox mechanism in DSSCs. The diffusion coefficient was calculated from the steady-state current (I_{ss}) using the following equation:

$$I_{ss} = 4nFDCr$$

where n is the number of electrons per molecule; F the Faraday constant; D the diffusion coefficient of I^{3-}; C is the bulk concentration of electroactive species; and r is the radius of the Pt ultra-microelectrode (5 μm).

Ionic conductivity was measured by AC impedance spectroscopy using a Solatron impedance analyzer (SI-1260) in combination with a potentiostat/ galvanostat electrochemical interface (SI-1286) in the frequency range 10 to 100 kHz at an AC amplitude of 10 mV, and a temperature of 25-90°C. The equipment was controlled using Z-Plot electrochemical software. Temperature-dependent ionic conductivity was processed by placing the electrochemical cell in an oven. The polymer electrolyte was melted into the electrochemical cell to form a structure of "steel | oligomer electrolyte | steel." Ionic conductivity σ was calculated according to the following equation:

$$\sigma = \frac{L}{A \cdot R_b}$$

where L is the thickness of the polymer electrolyte membrane, that is to say, the distance between the two stainless electrodes equal to 0.5 cm; A is the area of the electrode equal to 1 cm^2. Resistance (R_b) was taken at the intercept of the Nyquist plot with the real axis of the impedance spectra [imaginary (Z'') v.s. real (Z')].

2.4. Free volume analysis

Positron annihilation lifetime spectroscopy (PALS) measurements were performed by exposing the samples to radioactive ^{22}NaCl with an activity of 10μC. A fast-fast coincidence circuit with lifetime resolution of 240 ps, as monitored by a ^{60}Co source, was used to record all of the PALS spectra. The relaxation of excess free volume was calculated from the PALS data using the following equation:

$$\tau_{o-Ps} = \frac{1}{2}\left[1 - \frac{R}{R + \Delta R} + \frac{1}{2\pi}\sin\left(\frac{2\pi R}{R + \Delta R}\right)\right]^{-1}$$

where τ_{o-Ps} is given in nanoseconds and $\triangle R$ is the thickness of the homogeneous electron layer surrounding the free-volume hole where the P_s annihilates, such that $R_0 = R + \triangle R$ is the radius of the spherical potential wells corresponding to the free-volume hole [24].

2.5. Cell assembly and photo-electrochemical measurements

A TiO$_2$ photo-anode was deposited by screen-printing, to form double-layers of transparent and light-scattering films on the FTO glass plates (Solaronix). The total thickness of TiO$_2$ electrode was approximately 10 μm. The Pt catalyst was deposited on the FTO glass by drop-coating using H$_2$PtCl$_6$ solution (2 mg Pt in 1 ml ethanol) with repeated annealing at 400 °C for 15 minutes. The TiO$_2$ electrode was immersed in a 0.5 mM N719 dye solution in a mixture of acetonitrile and tert-butyl alcohol (volume ratio, 1:1), and maintained at room temperature for 24 hours to ensure complete uptake of the sensitizer. A 60 μm thick hot-melt sealing sheet (Solaronix) were used as a spacer. Details of the procedure involved in manufacturing TiO$_2$ photo-anode and Pt counter electrode and the assembly of cells has been described in another study [25]. DSSCs were investigated following the application of: 0.2M I$_2$, 0.1M LiI and 0.5M NMBI in the mixing matrix of PEGMEMA/PMII (v/v, 7:13).

2.6. 30 days long-term photo-electrochemical measurements

The cell described in Section 2.5 was placed into a glove box at room temperature, whereupon photovoltaic properties were measured with an AM 1.5 solar simulator equipped with a 450 W xenon lamp (Model N0.81172, Oriel) each day until the 30 day long-term testing procedure had been completed.

3. RESULTS AND DISCUSSION

3.1. Ionic conductivity and viscosity

Ionic conductivity is a critical factor in solar cell performance. The AC impedance method was used to determine the ionic composition, the concentration of tri-iodide ions, and the ionic conductivity of PEGMEMA oligomeric electrolytes as a function of the number of EO repeating units and temperature. Scheme 1 illustrates the effect of varying the EO repeat unit on ionic conductivity. From the scheme, we see that for oligomer 1, EO average repeat unit (n) = 2, oligomer 2, (n) = 4.5, and oligomer 3, (n) = 8.5. For temperatures between 25 ℃ and 90 ℃, ionic conductivity increased as the number of oligomer EO repeat units decreased. The increase in the number of EO groups was

detrimental to ionic conductivity, which could be explained by an increase in viscosity, which in turn resulted in an increase in molecular weight and intermolecular attractive forces within the structure of the electrolyte.

Table 1. Activation energy analysis of PEGMEMA oligomeric electrolytes at various temperatures.

	Oligomer 1	**Oligomer 2**	**Oligomer 3**
E_a (KJ mole^{-1})	32.2	40.3	41.6
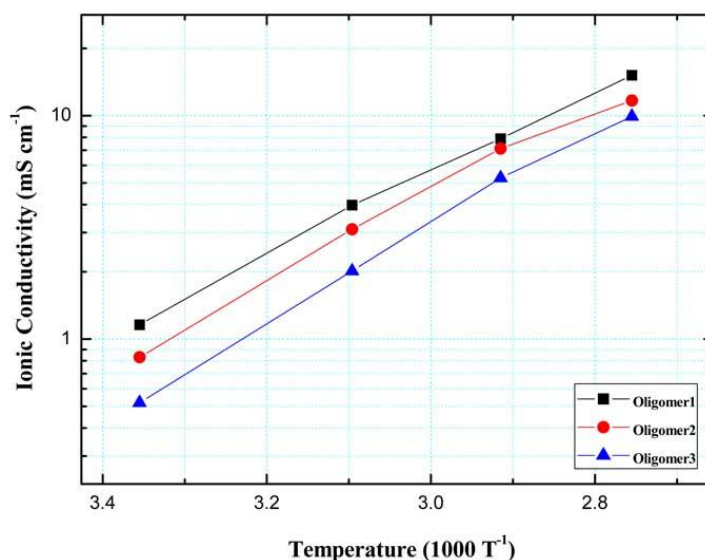
Figure 1. Ionic conductivity analysis of PEGMEMA oligomeric electrolytes at various temperatures.

According to Figure 1, an electrolyte with a flexible backbone and low viscosity could promote ionic transport. Observations regarding the maximum conductivity of oligomer 1, as $\sigma = 1.16 \times 10^{-3}$ S cm^{-1} at room temperature, and 15.17×10^{-3} S cm^{-1} at 90 ℃, are in agreement with conductivity values reported for quasi-solid state or gel polymer electrolytes [26, 27]. These plots are characteristic of an ion transport mechanism relying on the segmental motion of the EO repeat units in the backbone of the oligomer. We used the Vogel-Tamman-Fulcher (VTF) equation [28] to model the behavior of the temperature-dependent conductivity of these electrolytes according to three factors: parameters A, reflecting the number of charge carriers; B, the apparent activation energy; and T_0, the ideal glass transition temperature. The following VTF equation identifies the activation energy, E_a, of the ionic mobility, based on the assumption that the temperature dependence of conductivity, σ, demonstrates VTF behavior. The results are summarized in Table 1.

$$\sigma = AT^{-1/2} \exp\left(-B/R\,(T-T_0)\right)$$

This reveals that oligomer 1, with the lowest number of EO repeat units, had the lowest activation energy of 32.2 kJ mol^{-1}, and provided the highest ionic conductivity at room temperature. An increase in the molecular weight of the oligomer was accompanied by an increase in the viscosity of the electrolyte, and a low viscosity of approximately 6 cP (water is 1 cP) in oligomer 1. Following the addition of salts and PMII, the viscosity increased to approximately 170 cP; however, the viscosity of the oligomeric electrolytes doped with PMII was much lower than that of the solid polymer electrolyte.

Table 2. The viscosity of PEGMEMA oligomeric electrolytes at various temperature at a shear rate = 100 sec^{-1}.

	Viscosity (Pa-S)			
	Pure oligomer @ 25℃	25°C	50°C	90°C
Oligomer 1	0.006	0.17	0.05	0.03
Oligomer 2	0.007	0.37	0.07	0.03
Oligomer 3	0.025	0.57	0.10	0.03
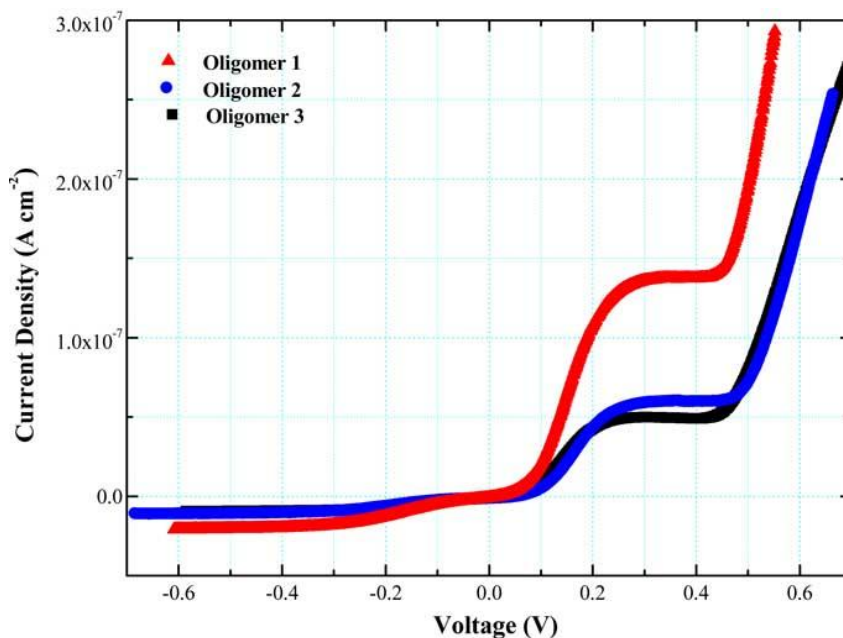
Figure 2. Linear steady-state voltammograms of PEGMEMA oligomeric electrolytes measured at a scan rate 10 mV sec^{-1}.

Table 2 illustrates the reduction in viscosity accompanying an increase in temperature. At 90 °C, all three of the oligomers approached similar conductivity values, suggesting that rapid side chain motion may overcome the effects of chain length, and this effect was particularly evident for oligomer 3. No other obvious physical changes were observed in the oligomer samples at high temperature.

3.2.Voltammetry and the diffusion coefficient

The ionic diffusion coefficient of tri-iodide was determined using an ultra-microelectrode technique, and Figure 2 shows linear, steady-state voltammograms of three oligomer electrolytes. As previously discussed, current density increased with a decrease in the length of the side-chain (containing EO groups). The lowest molecular weight of oligomer 1, had the shortest chain length, and provided enough free volume to allow ionic transfer for the redox couple $I^- | I^{3-}$, thereby increasing the degree of electrochemical reaction.

Table 3. Diffusion coefficients of triiodide and peak positions in steady-state voltammograms for PEGMEMA oligomer electrolytes.

	Diffusion coefficient ($* 10^{-7}$ cm^2 s^{-1})
	I_3^-
Oligomer 1	3.393 (0.39V)
Oligomer 2	1.486 (0.3V)
Oligomer 3	1.234 (0.3V)
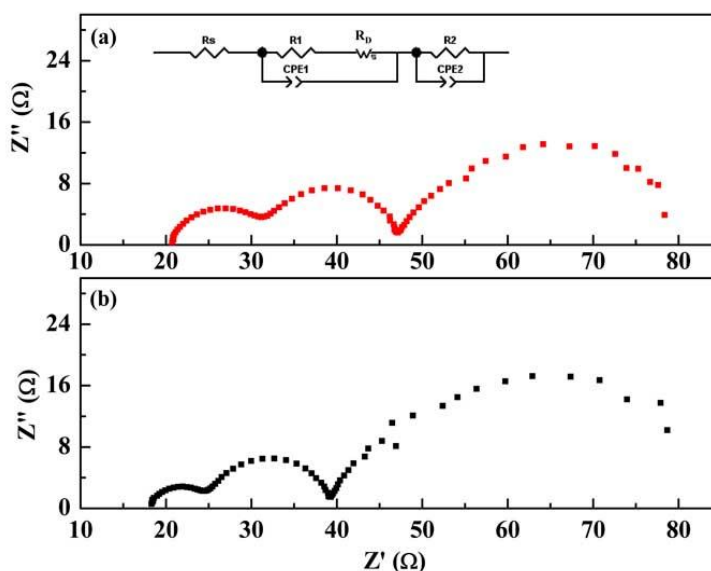
Figure. 3 I-V curves measured at 100 mW cm^{-2} of DSSCs employing PEGMEMA oligomeric electrolytes of various molecular weight.

Table 3 illustrates diffusion coefficients of the oligomers. As expected, oligomer 1 had the highest diffusion coefficient ($3.393*10^{-7}$ cm^2 s^{-1}), due to a higher molecular weight resulting from a three-dimensional restriction of ionic transfer. A higher tri-iodide diffusion coefficient resulted in a decrease in impedance in the ion diffusion process at the Pt electrode, because of an increase in the effective diffusion length and ionic migration velocity. However, the properties of the oligomeric

electrolyte differed greatly from those of volatile liquids, and the relatively small coefficient of our modified electrolyte represents a low transformation of the redox couple at the interface of the electrolyte and electrode.

In addition, the anodic reaction potential in Fig. 2 corresponds to a reduction in tri-iodide; as represented in the following [29-31]:

$$\text{Anodic Reaction 1 (-0.6~0V): } I_3^- + 2e^- \rightarrow 3I^-$$

$$\text{Anodic Reaction 2 (0~0.6V): } 3I^- - 2e^- \rightarrow I_3^-$$
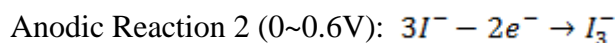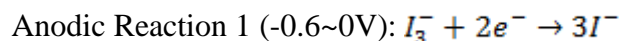
Accordingly, the tri-iodide reaction potential of oligomer 1 was assigned as 0.39V, due to the concentration and possible ohmic polarization caused by a decrease in viscosity, and increase in conductivity and diffusion coefficient compared with the other two oligomers. Oligomers 2 and 3 influenced polarization, with a corresponding effect on the advanced voltage (0.3V) in the test cell. This indicates that the molecular weight of the oligomer strongly influenced ionic transfer.

3.3.Electrochemical impedance spectroscopy

An equivalent circuit model of the internal elements of DSSC was constructed and divided into four regions. Figure 3 shows Nyquist plots for the electrochemical impedance spectroscopy of a DSSC using oligomer 1 with EMIBCN as the electrolyte, under 100 mW cm^{-2} measurement. The model in Fig. 3 exhibited similar behavior to the two DSSCs.

Series resistance (R_s) represents series primarily resistance in the electrolyte and wires. The first semicircle in the high frequency range was assigned as the charge transfer resistance (R_1) at the electrolytes/Pt interface. The second semicircle represents the resistance (R_2) of photo-injected electrons within the DSSC TiO$_2$ layer. The last semicircle, in the low frequency region, represents the electrolyte diffusion impedance (R_D) of the redox couple at the surface of the Pt.

Table 4. Performance characteristics of DSSCs employing PEGMEMA oligomeric electrolytes at 100 mW cm^{-2}.

	R_S (Ω)	R_1 (Ω)	R_D (Ω)	R_2 (Ω)	τ (s)	d (μm)
Oligomer 1	20.66	12.19	34.5	14.15	9.07	10.3
EMIBCN	18.03	6.85	42.5	13.4	13.35	13.7
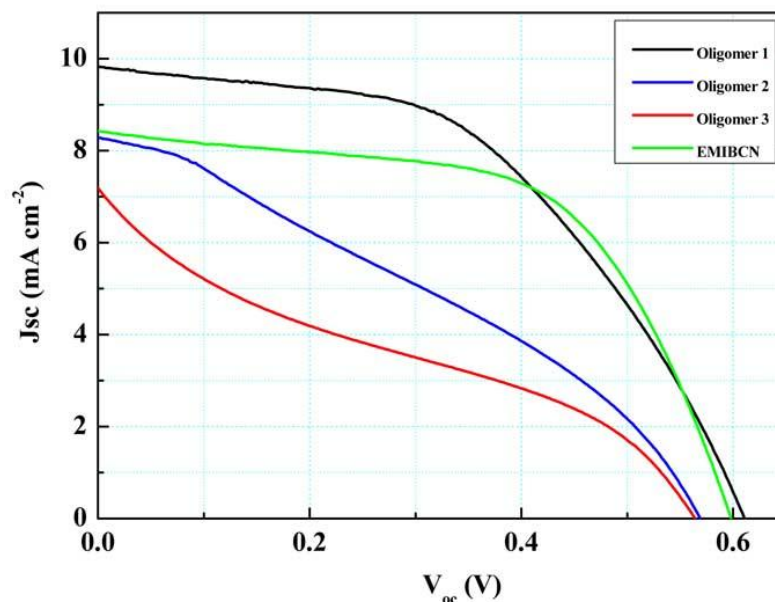
Figure 4. Positron lifetime distribution and free volume of micro voids in PEGMEMA oligomeric electrolytes with EO of various lengths.

Table 4 shows these values after the simulation. The main difference is seen in the value for R_S, relative to the ionic conductivity of electrolytes. EMIBCN provided lower R_s resistance than oligomer 1 did, indicating that the ionic conductivity of EMIBCN exceeded that of oligomer 1. The resistance of R_1 indicates that EMIBCN had nearly half of the charge transfer resistance as that of oligomer 1. The reason for this was the improved interfacial contact between the Pt counter electrode and the electrolyte (EMIBCN), providing a soft, flexible molecular construction that benefited the transfer of ions. The value of R_2 indicates that EMIBCN provided superior contact with the TiO_2, but the difference between R_1 and R_2 was not great, because the polarization of oligomer 1 was very similar to that of TiO_2. However, the difference in diffusion resistance of acrylate-substituted functional groups, and the EO groups of oligomer 1 suggest that an improvement in ionic diffusion on the surface of the Pt was due to an enhancement of the ionic transport by the EO to a greater degree than that provided by EMIBCN. This is important, because the migration of the redox couple through the bulk electrolyte and the interface becomes easier with the coordination of lithium cations by the EO, thereby reducing resistance. The diffusion distance (d) and time constant (τ) of redox couple on the Pt surface are provided by the following two equations [32],

$$R_{D(f)} = R_{D(0)} \left\{ \frac{\tanh \sqrt{j\omega\tau}}{\sqrt{j\omega\tau}} \right\}$$

$$\frac{1}{\tau} = D \times d^{-2}$$

According to the time constant results of oligomer 1 (9.07 s) and EMIBCN (13.35 s), the EO ionic enhancement is confirmed by the lower value seen in τ compared to EMIBCN, which lacks the EO electron-withdrawing group.

3.4. Comparison of Oligomer Photovoltaic (PV) Performance

Figure 4 shows *I-V* curves for the three oligomers related to EO ionic transfer effects under AM 1.5 illumination. The cell using oligomer 1 produced the highest current density at 9.83 mA cm^{-2}, and open-circuit voltage of 0.61V, compared to the other two oligomers. This performance could be attributed to the high diffusion coefficient of the redox couple, high ionic conductivity, and low viscosity.

Table 5. o-Ps lifetime parameters of PEGMEMA oligomeric electrolytes depend on the length of side chain.

	J_{sc} (mA cm^{-2})	V_{oc} (V)	ff (%)	η (%)
Oligomer 1	9.83	0.61	0.50	2.99
Oligomer 2	8.29	0.57	0.33	1.58
Oligomer 3	7.13	0.57	0.23	1.15
EMIBCN	8.57	0.60	0.59	3.02
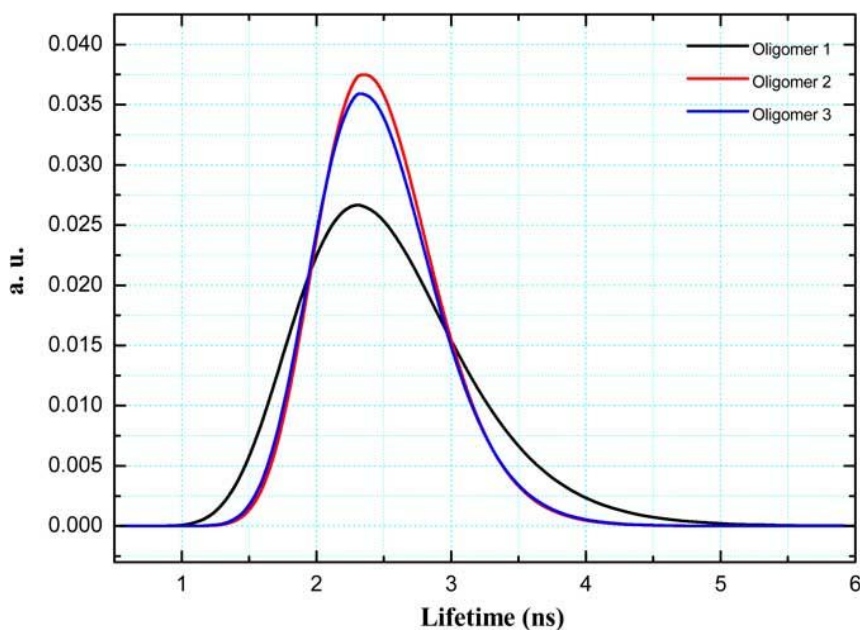
Figure 5. Electrochemical impedance spectra of DSSCs based on (a) oligomer 1 and (b) EMIBCN electrolytes.

Table 5 shows that the open-circuit voltage of the three oligomeric electrolytes and EMIBCN were all approximately 0.6 V for the same concentration of iodide salts. The overall conversion efficiency achieved for oligomer 1 was 2.99%, which was very close to that of the cell produced by Gratzel's using EMIBCN [23]. In addition, the J_{sc} of oligomer 1 (9.83 mA cm^{-2}) was far higher than that of EMIBCN system (8.57 mA cm^{-2}), suggesting an improvement in ionic diffusion on the surface of the Pt due to the EO ionic assistance of the oligomer electrolyte. The use of a thin TiO$_2$ film on the photo-electrodes restricted the quantity of dye that could be absorbed. In Section 3.6, we discuss the investigation into the effect of using a thinner spacer. The baseline performance, as established by an AN-based electrolyte using the same cell as that in Table 5, far exceeded all experimental samples including oligomers and EMIBCN.

3.5. Free volume

Positron-annihilation lifetime-spectroscopy (PALS) is a well established and highly sensitive technique for probing sub-nanometer sized local free-volumes in amorphous polymers [33].

Table 6. Numerical values for some elements calculated from fitting on DSSCs for oligomer 1 and EMIBCN.

Sample	R(Å)	fv(Å^3)	ffv(%)
Oligomer 1	3.19	136.4	1.79
Oligomer 2	3.15	135.2	1.78
Oligomer 3	3.12	134.0	1.77
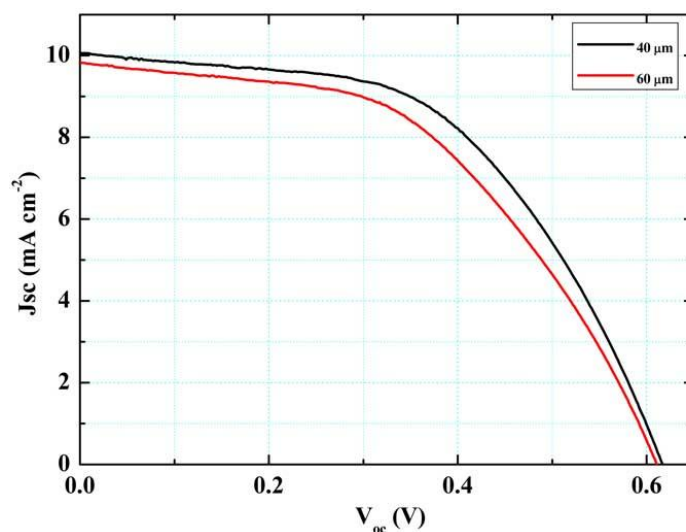
Figure 6. I-V curves measured at 100 mWcm^{-2} of DSSCs employing oligomer 1 electrolyte with 40 μm and 60 μm thickness spacers.

Figure 5 lists the results of free volume evaluation of the oligomeric electrolytes with respect to the orthopositronium lifetime, T_{oPs}, as a function of the lengths of the EO chains in these oligomer electrolytes. The results show that the T_{oPs} was nearly constant, with an increase in the number of EO functional groups, indicating that the average size of the free volume holes was constant. The diameter of the hole (R), free volume (fv), and totally free volume occupied content (ffv) are shown in Table 6. The results show an extremely tiny inverse proportion to chain length, revealing that the length of the EO definitely influenced the route of the ionic transfer.

This illustrates the dependence of these oligomeric electrolytes on the presence of EO. Another interesting behavior was also observed in Fig. 5, in which oligomer 1 exhibited a dramatic difference in its short and broad integrated area compared to oligomers 2 and 3, which typically present a lifespan in the regions of 1~2 ns or 3~5 ns. Under PALS theory, a shorter lifespan suggests smaller free volume holes, and a large lifespan suggests larger free volume holes. Thus, the PALS spectra should be able to determine whether the ionic radii of the redox couple was compatible with the available holes. If the PALS lifespan of oligomer 1 was determined to have a better fit with the free volume space than the remaining oligomers, then this would explain the better cell performance observed with this oligomer.

3.6. Photovoltaic performance of spacer effects

Section 3.5 illustrates the unique ionic transfer properties of oligomer 1, related to free volume. Due to these ionic transfer properties, a thinner spacer was applied to validate the relationship between ionic transfer and cell performance employing the same oligomer electrolyte.

Table 7. Performance characteristics of DSSCs employing oligomer 1 electrolytes with different thickness spacer at 100 mW cm^{-2}

Thickness (μm)	J_{sc} (mA cm^{-2})	V_{oc} (V)	ff (%)	η (%)
40	10.07	0.62	0.53	3.29
60	9.83	0.61	0.5	2.99

Figure 6 and Table 7 show the *I-V* curves for spacers of various thicknesses. The short-circuit photocurrent density, J_{sc}, open-circuit photovoltage (V_{oc}), and fill factor (FF) of the cell with the oligomer 1 electrolyte were examined at 10.07 mA cm^{-2}, 0.62 V, and 0.53 for the 40 μm spacer, yielding an improvement in photovoltaic conversion efficiency of 3.29%, compared with that of the 60 μm layer.

This reveals that the ionic transfer route was shortened using a thinner spacer, which effectively assisted the movement of the ions through oligomer 1, thereby improving the performance of the photocell. In addition, oligomers 2 and 3 did not show significantly improvements after the spacer had been replaced. This is a clear verification of the free volume results.

3.7. Long term stability

To estimate the effect of the viscosity of the oligomeric electrolytes, a 30-day test was conducted at room temperature. This test was conducted to determine the penetration of the oligomer into the TiO_2 crystalline layer and validate the long-term stability of the cells.
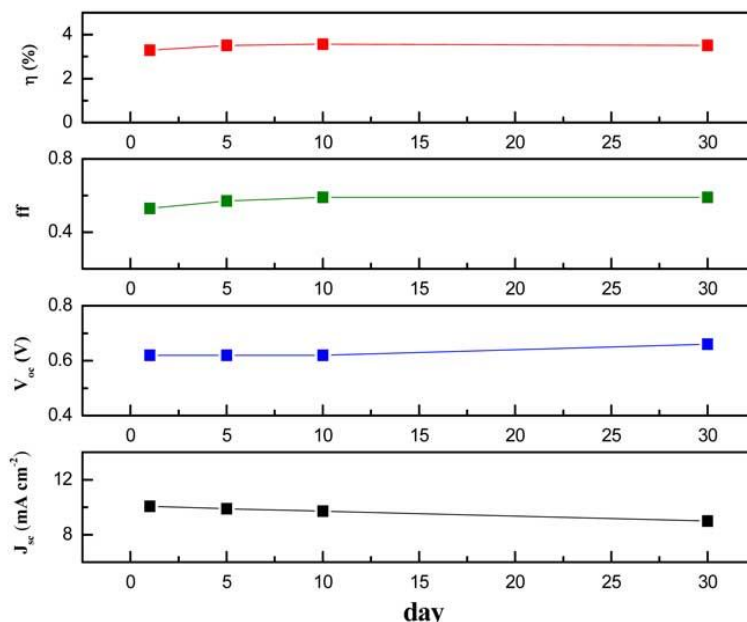
Figure 7. 30 days evaluation of long-term stability of DSSC employing oligomer 1 electrolyte at room temperature.

Figure 7 illustrates the short-circuit photocurrent density (J_{sc}), open-circuit photovoltage (V_{oc}), and fill factor (FF) of the cell after the 30 day long-term test using oligomer 1.The electrolyte achieved $J_{sc} = 9.71$ mA cm^{-2}, $V_{oc} = 0.62$ V, and FF = 0.59, and an excellent photovoltaic conversion efficiency of 3.56% throughout the 30 day test. According to the improvement in cell efficiency following the long-term test, the oligomeric electrolyte was confirmed to have penetrated into the TiO_2, indicating that the new PEGMEMA oligomeric electrolytes provides high performance operation with excellent cell stability for next generation DSSC applications.

4 CONCLUSION

In this paper, we obtained an excellent 3.56% energy conversion at AM 1.5, comparable to other solvent-free systems. This kind of PEGMEMA oligomeric electrolyte possesses a number of advantages such as low cost, simple production, high cell performance, and stability. We determined that both ionic conductivity and viscosity, as well as the diffusion coefficients of tri-iodide are greatly influenced by oligomers with side chains of varying lengths containing the EO functional group. In addition, the free volume results of oligomeric electrolyte indicates that ionic transfer significantly

influences cell performance. Moreover, the requirements of cells and the composition of PEGMEMA oligomeric electrolytes have yet to be optimized, providing considerable room for improvement in the performance of cells. Even still, oligomer 1 (PEGMEMA$_{188}$) electrolyte is recommended right now as a potential candidate for solvent-free electrolytes in DSSCs.

References

1. M. Grätzel, *Nature* 414 (2001) 338-344
2. D. Soundararajan, J. K. Yoon, Y. I. Kim, J. S. Kwon, C.W. Park, S. H. Kim, J. M. Ko, *Int. J. Electrochem. Sci.* 4 (2009) 1628-1637
3. H. Karami, A. Kaboli, *Int. J. Electrochem. Sci.,* 5 (2010) 706-719
4. J. M. Kroon, H. J. P. Smit, P. Liska, K. R. Thampi, P. Wang, S. M. Zakeeruddin, M. Grätzel, A. Hinsch, S. Hore, U.Würfel, R. Sastrawan, J. R. Durrant, E. Palomares, H. Pettersson, T. Gruszecki, J. Walter, K. Skupien, G. E. Tulloch, *Prog, Photovolt: Res. Appl.* 15 (2007) 1-18
5. M. Gorlov, H. Pettersson, A. Hagfeldt, L. Kloo, *Inorg. Chem.* 46 (2007) 3566-3575
6. S. Y. An, I. C. Jeong, M. -S. Won, E. D. Jeong, Y. -B. Shim, *J. Appl. Electrochem.* 39 (2009) 1573-1578
7. Q. Xiao, X. Wang, W. Li, Z. Li, T. Zhang, H. Zhang, *J. Mem. Science* 334 (2009)117-122
8. J. Zhang, H. Han, S. Wu, S. Xu, Y. Yang, C. Zhou, X. Zhao, *Solid State Ionics* 178 (2007) 1595-1601
9. J. Zhang, H. Han, S. Wu, S. Xu, C. Zhou, Y. Yang, X. Zhao, *Nanotechnology* 18 (2007) 295606
10. C. W. Lin, C. L. Hung, M. Venkateswarlu, B. J. Hwang, *J. Power Sources* 146 (2005) 397-401
11. L. Hu, Z. Tang, Z. Zhang, *J. Power Sources* 66 (2007) 226-232
12. G. Jiang, S. Maeda, Y. Saito, S. Tanase, T. Sakai, *J. Electrochem. Soc.* 152 (2005) A767-773
13. F. Croce, G. B. Appetecchi, L. Persi, B. Scrosati, *Nature* 394 (1998) 456-458
14. M. Watanabe, A. Nishimoto, *Solid State Ionics* 79 (1995) 306-310
15. J. H. Park, K. J. Choi, J. Kim, Y. S. Kang, S. S. Lee, *J. Power Sources* 173 (2007) 1029-1033
16. M. Gorlov, L. Kloo, *Dalton Transactions* 20 (2008) 2655-2666
17. N. Yamanaka, R. Kawano, W. Kubo, N. Masaki, T. Kitamura, Y. Wada, M. Watanabe, S. Yanagida, *J. Phys. Chem. B* 111 (2007) 4763-4769
18. F. M. Wang, C. C. Wan, Y. Y. Wang, *J. Appl. Electrochem.* 39 (2009) 253-260
19. F. M. Wang, C. C. Hu, S. C. Lo, Y. Y. Wang, C. C. Wan, *Solid State Ionics* 180 (2009) 405-411
20. F. M. Wang, C. C. Hu, S. C. Lo, Y. Y. Wang, C. C. Wan, *J. Electroanal. Chem.* 644 (2010) 25-29
21. F. M. Wang, D. T. Shieh, J. H. Cheng, C. R. Yang, *Solid State Ionics* 180 (2010) 1660-1666
22. F. M. Wang, H. C. Wu, C. S. Cheng, C. L. Huang, C. R. Yang, *Electrochimica Acta* 54 (2009) 3788-3793
23. D. Kuang, S. Ito, S. M. Zakeeruddin, M. Gratzel, *J. Am. Chem. Soc* 128 (2006) 7732-7733.
24. M. A. Monge, J. A. Dı´az, R. Pareja, *Macromolecules* 37 (2004) 7223-7227
25. S. Ito, P. Comte, P. Liska, C. Grätzel, M. K. Nazeeruddin, M. Grätzel, *Thin Solid Films* 516 (2008) 4613-4619
26. D. Saikia, C. C. Han, Y. W. C. Yang, *J. Power Sources* 185 (2008) 570-576
27. D. W. Kim., Y. B. Jeong, S. H. Kim, D. Y. Lee, J. S. Song, *J. Power Sources* 149 (2005) 112-116
28. N. Binesh, S. Bhat, *J. Polymer Science B* : *Polymer Physics* 36 (1998) 1201-1209

29. V. A. Macagno, *Electrochemica. Acta* 11 (1966) 1553–1557
30. Y. Bai, Y. C., J. Zhang, M. Wang, R. Li, P. Wang, S. M. Zakeeruddin, M. Gratzel, *Nature Materials* 7 (2008) 626-630
31. P. Wang, Q. Dai, S. M. Zakeeruddin, M. Forsyth, D. R. MacFarlane, M. Gratzel, *J. Am. Chem. Soc.* 126 (2004) 13590-13591
32. M. E. Orazem, B. Tribollet, Electrochemical Impedance Spectroscopy, first ed., John Wiley & Sons, Inc., New Jersey, 2008.
33. M. Eldrup, D. Lightbody, J. N. Sherwood, *Chem. Phys.* 63 (1981) 51-58.